Simulation of Topology Optimized Electrothermal Microgrippers

O. Sardan[*,1], D. H. Petersen[1], O. Sigmund[2] and P. Bøggild[1]
[1]DTU Nanotech, Denmark
[2]DTU Mechanical Engineering, Denmark
*Corresponding author: DTU Nanotech, Ørsteds Plads, DTU Building 345E, DK-2800, Kgs. Lyngby, Denmark, oezlem.sardan@nanotech.dtu.dk

Abstract: In this work, electrothermal microgrippers designed using topology optimization are modeled. The microgrippers are composed of two 5 μm-thick polysilicon actuators facing each other. The gap between the actuators are 2 μm in the initial state and the microgrippers are able to both fully close and further open this gap. The operation principle of the actuators is quite similar to that of a parallel-beam electrothermal actuator and relies on resistive heating by passing a current through the structure. COMSOL MEMS Module is used in order to model the temperature distribution, end-effector displacement and stiffness of both topology optimized and conventional parallel-beam actuators. End-effector displacement vs. bias voltage curves for both modes, i.e. open and close, of the microgrippers obtained through finite element analysis fit almost perfectly to the experimental data.

Keywords: Microgrippers, electrothermal actuators, topology optimization.

1. Introduction

Electrothermal microgrippers are promising tools enabling manipulation and assembly of nano-scale structures, which is rather challenging. A simple type of an electrothermal microgripper is composed of two parallel-beam actuators (Figure 1 (left)) [1, 2]. Parallel-beam opposing microgrippers are advantageous due to their compactness, design flexibility and operational simplicity.

The most important performance criteria for electrothermal microgrippers can be listed as the actuator force, the actuation range and the temperature of the end-effectors during actuation. Although parallel beam microgrippers have a relatively large actuation range, they are on the lower limit of supplying sufficient force to detach nano-structures which are firmly attached to a substrate surface [2], such as vertically grown carbon nanotubes (CNTs) [3]. Furthermore, the temperature of the end-effectors during actuation is quite high, enabling only manipulation of nanostructures with a high melting temperature.

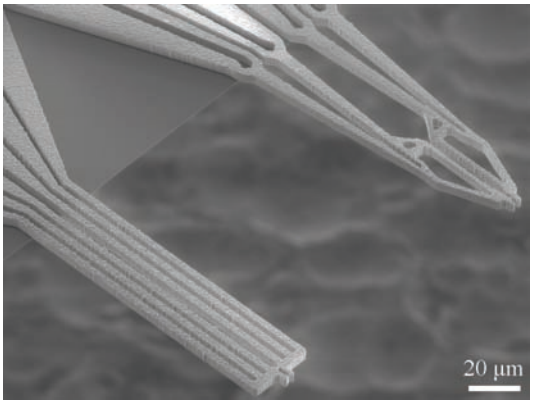

Figure 1. Electrothermal microgrippers: a parallel-beam (left) and a topology optimized (right) design.

We decided to use topology optimization in order to design electrothermal microgrippers with the highest possible actuator force at the desired actuation range and the lowest possible operation temperature. Topology optimization is a finite element based method, which relies on distribution of a certain amount of material within a well-defined design domain to perform a specific task [4].

In this paper, topology optimized electrothermal microgrippers and their operation principle are introduced initially. Then, the procedure for the finite element analysis performed using COMSOL MEMS Module is described in detail, mentioning about the 3D model and the simulation settings. Finally, the results of the finite element simulations are discussed, together with their comparison with the experimental data.

2. Topology Optimized Microgrippers

Electrothermal microgrippers were designed using topology optimization and they were fabricated from a 5 μm-thick highly boron-doped

polysilicon device layer with a 1 μm-thick buried silicon dioxide layer separating the device layer from the silicon handle wafer (Figure 1 (right)). Detailed design and fabrication procedures can be found elsewhere [5].

The operation principle of the topology optimized microgrippers is the same as that of a parallel beam microgripper, which relies on resistive heating of the structure by passing a current through it (Figure 2). The microgrippers can both open and close depending on the configuration of the voltages applied to the actuator beams.

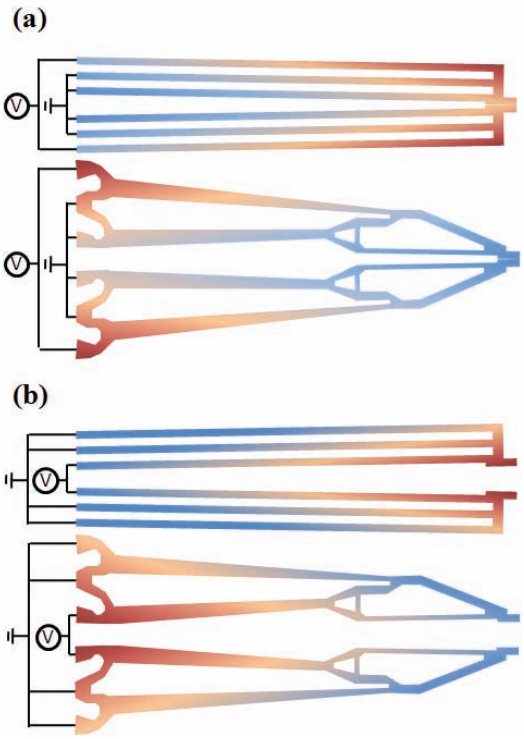

Figure 2. Operation principle of parallel-beam and topology optimized microgrippers showing the voltage configuration for (a) closing and (b) opening modes.

According to the results of the optimization algorithm, the topology optimized actuator is an order of magnitude stronger than that a three-beam actuator. However, mechanical properties of the actual devices are expected to be different as a result of the deviation from the original design during conversion of the gray-scale output of the topology optimization program to a binary image (see [5]). Such changes may also yield to a difference in the operation temperature of the actuator. Hence, performing finite element analysis of the topology optimized actuator prior to fabrication is of vital importance for predicting the performance of the fabricated devices.

3. Finite Element Simulations

Finite element simulations of the topology optimized actuator were performed using the MEMS Module of COMSOL 3.4. The model was composed of three application modes: Conductive Media DC (emdc), Heat Transfer by Conduction (ht) and Solid, Stress-Strain (smsld).

3.1 Geometry Settings

The workplane was selected as z=0 and a 2D CAD drawing of the topology optimized actuator was imported from a DXF file. The 3D model was then created by extruding the imported geometry along the z-axis. In addition to the actuator itself, the first 100 μm length of the leads connecting the device to the contact pads were also included in the model, together with the 1 μm-thick silicon dioxide layer underneath them (Figure 3).

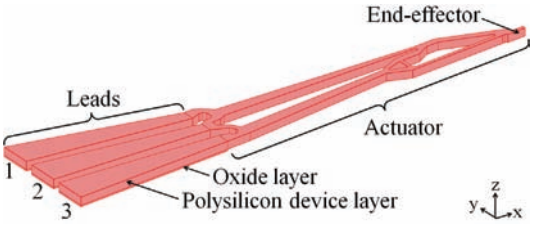

Figure 3. The 3D COMSOL model for the topology optimized actuator.

3.2 Subdomain Settings

Materials for the polysilicon and silicon dioxide layers were selected from the materials library of COMSOL MEMS Module as “poly-Si” and “SiO2”, respectively. However, coefficient of thermal expansion and electrical and thermal conductivities of polysilicon were changed and defined asappropriate functions of temperature [6] (Appendix 8.1 & 2).

In the Heat Transfer by Conduction application mode, a heat source was defined with the value “Q_dc”, which corresponds to the

resistive heating calculated during the electrical analysis. Also the initial temperature was set to 300 K for all subdomains in this application mode.

In the Solid, Stress-Strain application mode, and under the "Load" tab, the thermal expansion was included by defining the strain temperature as "T" and the strain reference temperatures as 300 K. Here, "T" is the temperature calculated during the thermal analysis.

3.3 Boundary Settings

Boundary settings for the electro-thermomechanical simulation of the closing mode of the microgrippers were as follows:

In the Conductive Media DC application mode, electric potential boundary conditions were applied to the ends of the polysilicon leads (Figure 3). For this mode, Lead 1 was set to an electric potential of "V0" and Leads 2 & 3 were defined as "Ground". All remaining boundaries were defined as "Electric Insulation".

In the Heat Transfer by Conduction application mode, temperature boundary conditions were applied to the bottom of the oxide layers underneath the leads (Figure 3) by setting all three to 300 K. Also, the effect of heat transfer through the air was included by defining a heat flux boundary condition to all boundaries, which are in contact with air. External temperature for the heat flux is defined as 300 K and a temperature dependent heat transfer coefficient was used [6] (Appendix 8.2). All remaining boundaries were defined as "Thermal Insulation".

In the Solid, Stress-Strain application mode, the bottom surfaces of the oxide layers underneath the leads were defined as "Fixed", where the remaining boundaries were defined as "Free".

Boundary settings for the opening mode of the microgrippers were the same as those for the closing mode, except the boundary conditions for Leads 1 & 3 are interchanged (Figure 2).

Finally, only a mechanical simulation of the microgrippers was performed in order to calculate the structural stiffness of the actuators. Mechanical boundary conditions for this simulation were the same as both opening and closing modes, except that a prescribed displacement of 1 μm along y-direction was applied to the end-effector boundary (Figure 3).

3.4 Mesh Settings

Since heater and end-effector locations are the most critical regions of the topology optimized actuator, a variable mesh density was used when meshing the structure and a smaller mesh size was used at these locations (Figure 4).

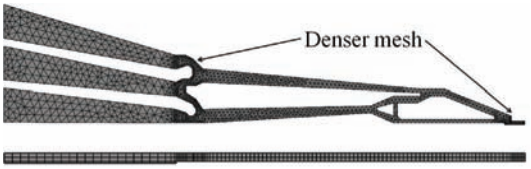

Figure 4. Meshed model: top (top) and side views (bottom).

In the Free Mesh Parameters menu, the edges at the heater and end-effector locations were meshed with a maximum element size of 1 μm. Then, top surfaces of the actuator and the leads were meshed with maximum element sizes of 2.5 μm and 5 μm, respectively. Finally, in the Swept Mesh Parameters menu, the meshes created on the top surfaces were swept along z-direction, using 2 and 1 element layers for polysilicon and oxide subdomains, respectively.

3.5 Solver Settings

The electrothermomechanical simulations of the microgrippers were performed using the parametric solver and the parameter "V0" was solved for values from 0.5 to 6 V with 0.5 V steps. The mechanical simulation of the microgrippers was performed using the stationary solver. The linear system solver is selected as "Direct (PARDISO)" for all cases.

4. Results and Discussion

Results for the temperature distribution within the topology optimized actuator at 1 μm displacement for both closing and opening modes are plotted in Figure 5, where the end-effector temperatures are 265 °C and 371 °C, respectively.

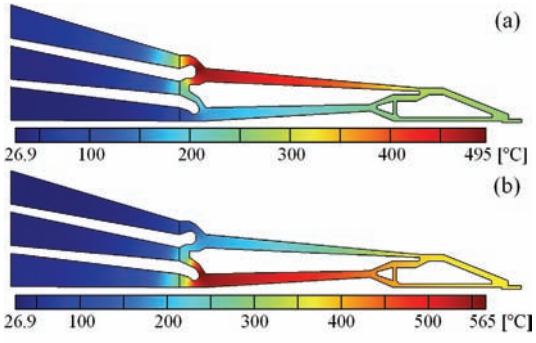

Figure 5. Simulation results for the temperature distribution within the topology optimized actuator at 1 μm displacement in (a) closing and (b) opening modes.

Actuation curves obtained experimentally are compared with the simulation results in Figure 6, where the experimental voltage was normalized to fit the simulation. This is done to account for interconnects serial resistance in the experimental setup.

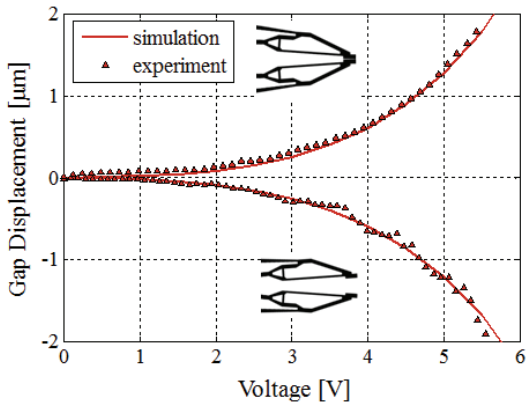

Figure 6. Comparison of the experiment results with finite element simulations for the gap displacement vs. bias curves for the topology optimized microgrippers.

Stiffness of the actuator was calculated as 235 N/m, by integrating the y-component of the force acting on the end-effector boundary, i.e., "lm4", at a displacement of 1 μm along the y-direction.

5. Conclusions

The simulation results seem credible as the displacement behavior of the topology optimized actuator fits quite well with the experimental data. Such an analysis is quite useful for predicting the maximum operation voltage as well as the end-effector temperature and the temperature distribution within the actuator. These parameters are rather important for selecting an appropriate gripper design for a specific type of sample to be manipulated.

The stiffness value calculated according to the mechanical simulation is much higher than that expected by the topology optimization algorithm [5]. The reason for this difference is the change in the mechanical properties of the device during various design steps (see Sect. 2).

In order to verify the correctness of the simulations, the same mechanical simulation was also performed for the 3-beam actuator. According to the results of this simulation, the stiffness of the 3-beam actuator is calculated as 2.2 N/m, which is the same as the theoretical value calculated using the formula given in [1].

6. References

1. K. Mølhave and O. Hansen, Electro-thermally actuated microgrippers with integrated force feedback, *J. Micromech. Microeng.*, **15**, 1265–70 (2005).
2. K.N. Andersen, D.H. Petersen, K. Carlson, K. Mølhave, O. Sardan, A. Horsewell, V. Eichhorn, S. Fatikow and P. Bøggild, Multimodal electrothermal silicon microgrippers for nanotube manipulation, *Paper accepted by IEEE Trans. Nanotechnol.* (2008).
3. K.B.K. Teo, S-B. Lee, M. Chhowalla, V. Semet, V.T. Binh, M. Castignolles, A. Loiseau, G. Pirio, P. Legagneux, D. Pribat, D.G. Hasko, H. Ahmed, G.A.J. Amaratunga and W.I. Milne, Plasma enhanced chemical vapour deposition carbon nanotubes/nanofibres—how uniform do they grow?, *Nanotechnology*, **14**, 204-11 (2003).
4. M.P. Bendsøe and O. Sigmund, Topology Optimization, Theory Methods and Applications, 2nd Ed., Springer Verlag, Berlin, Heidelberg (2003).
5. O. Sardan, D.H. Petersen, K. Mølhave, O. Sigmund and P. Bøggild, Topology optimized electrothermal polysilicon microgrippers, *Microelectron. Eng.*, **85 (5-6)**, 1096-9 (2008).
6. A.A. Geisberger, N. Sarkar, M. Ellis and G.D. Skidmore, Electrothermal Properties and Modeling of Polysilicon Microthermal Actuators, *J. Microelectromech. Syst.*, **12 (4)**, 513–22 (2003).

7. Acknowledgements

This project is supported by the EU grants NANOHAND (IP 034274) and NANORAC (STREP 013680).

Authors would like to Lars Gregersen and Thure Ralfs from COMSOL A/S for their assistance.

8. Appendix

8.1 Material Properties of Polysilicon

Table 1: Thermal conductivity and coefficient of thermal expansion values of polysilicon [6].

Temperature [K]	Thermal Conductivity [W/(m·K)]	CTE [K^{-1}]
300	65.00	2.5×10^{-6}
400	53.75	3.1×10^{-6}
500	46.54	3.5×10^{-6}
600	40.00	3.8×10^{-6}
700	35.00	4.1×10^{-6}
800	32.08	4.3×10^{-6}

8.2 Functions

Table 2: Function for the electrical resistivity of polysilicon [6].

$1/\rho = \alpha_{1+} \alpha_2 . T^{\alpha 3}$	
Coefficient	Value
α_1	2.6×10^{-3}
α_2	8.16×10^{-9}
α_3	1.946

Table 3: Heat transfer coefficient for air [6].

Temperature [K]	Heat Transfer Coefficient [$W/(m^2 \cdot K)$]
300	1101.7
400	1214.3
500	1381.0
600	1520.7
700	1660.3
800	1799.9